The Astrophysical Journal Supplement Series, 238:30 (10pp), 2018 October https://doi.org/10.3847/1538-4365/aadf81


# LAMOST Observations in the *Kepler* Field. II. Database of the Low-resolution Spectra from the Five-year Regular Survey*

Weikai Zong[1], Jian-Ning Fu[1,12], Peter De Cat[2], Jianrong Shi[3], Ali Luo[3], Haotong Zhang[3], A. Frasca[4], C. J. Corbally[5], J. Molenda- Żakowicz[6], G. Catanzaro[4], R. O. Gray[7], Jiangtao Wang[1], Yang Pan[1], Anbing Ren[1], Ruyuan Zhang[1], Mengqi Jin[1], Yue Wu[3], Subo Dong[8], Ji-Wei Xie[9,10], Wei Zhang[3], and Yonghui Hou[11]
LAMOST-Kepler collaboration
[1] Department of Astronomy, Beijing Normal University, Beijing 100875, People's Republic of China; jnfu@bnu.edu.cn
[2] Royal Observatory of Belgium, Ringlaan 3, B-1180 Brussel, Belgium
[3] Key Lab for Optical Astronomy, National Astronomical Observatories, Chinese Academy of Sciences, Beijing 100012, People's Republic of China
[4] INAF—Osservatorio Astrofisico di Catania, Via S. Sofia 78, I-95123 Catania, Italy
[5] Vatican Observatory Research Group, Steward Observatory, Tucson, AZ 85721-0065, USA
[6] Astronomical Institute of the University of Wrocław, ul. Kopernika 11, 51-622 Wrocław, Poland
[7] Department of Physics and Astronomy, Appalachian State University, Boone, NC 28608, USA
[8] Kavli Institute for Astronomy and Astrophysics, Peking University, Yi He Yuan Road 5, Hai Dian District, Beijing, 100871, People's Republic of China
[9] School of Astronomy and Space Science, Nanjing University, Nanjing 210093, People's Republic of China
[10] Key Laboratory of Modern Astronomy and Astrophysics in Ministry of Education, Nanjing University, Nanjing 210093, People's Republic of China
[11] Nanjing Institute of Astronomical Optics & Technology, National Astronomical Observatories, Chinese Academy of Sciences, Nanjing 210042, People's Republic of China
*Received 2018 June 8; revised 2018 August 25; accepted 2018 August 31; published 2018 October 15*

## Abstract

The LAMOST-*Kepler* (LK-) project was initiated to use the Large Sky Area Multi-Object Fiber Spectroscopic Telescope (LAMOST) to make spectroscopic follow-up observations for the targets in the field of the *Kepler* mission. The *Kepler* field is divided into 14 subfields that are adapted to the LAMOST circular field with a diameter of 5°. During the regular survey phase of LAMOST, the LK-project took data from 2012 June to 2017 June and covered all 14 subfields at least twice. In particular, we describe in this paper the second Data Release of the LK-project, including all spectra acquired through 2015 May–2017 June together with the first round observations of the LK-project from 2012 June to 2014 September. The LK-project now counts 227,870 spectra of 156,390 stars, among which we have derived atmospheric parameters ($\log g$, $T_{\rm eff}$, and [Fe/H]) and heliocentric radial velocity for 173,971 spectra of 126,172 stars. These parameters were obtained with the most recent version of the LAMOST Stellar Parameter Pipeline v 2.9.7. Nearly one half, namely 76,283 targets, are observed both by the LAMOST and *Kepler* telescopes. These spectra, establishing a large spectroscopy library, will be useful for the entire astronomical community, particularly for planetary science and stellar variability on *Kepler* targets.

*Key words:* astronomical databases: miscellaneous – stars: fundamental parameters – stars: general – stars: statistics – techniques: spectroscopic

## 1. Introduction

The *Kepler* satellite was launched on 2009 March 7th by *NASA* with the aim of searching for Earth-sized planets around solar-like stars (Borucki et al. 2010). Before its second of four reaction wheels on board failed on 2013 May 11th, *Kepler* had been continuously monitoring about 200,000 stars together within a 105 deg$^2$ field in the constellations Cygnus and Lyrae region for a period of ∼4 years. These unprecedented high-quality photometric data are gold mines for the field of asteroseismology (Gilliland et al. 2010), as well as for many other scientific interests (see, e.g., eclipsing binaries in Prša et al. 2011). Nevertheless, to uncover in-depth physics for interesting targets with *Kepler* photometry, it is crucial that the input atmospheric parameters of stars are available beforehand, as successful asteroseismology depends somewhat on the effective temperature ($T_{\rm eff}$), surface gravity ($\log g$), and metallicity ([$M/H$]), measured first from spectroscopy, that could reduce the size of parameter space to find the optimal seismic models (see, e.g., Cunha et al. 2007; Charpinet et al. 2011). The Kepler Input Catalog (KIC; Brown et al. 2011) provides the stellar parameters of potential interesting targets that are derived mainly from photometry in the SDSS-like photometric bands (Doi et al. 2010), but the precision of KIC is not high enough for asteroseismic modeling, particularly for hot and peculiar stars (Molenda-Żakowicz et al. 2011; McNamara et al. 2012; Huber et al. 2014). There are many additional endeavors to improve the precision of atmosphere parameters for seismic aims with ground-based spectroscopic data (see, e.g., Uytterhoeven et al. 2010; Thygesen et al. 2012; Niemczura et al. 2015). It is inevitable that these projects are not allocated sufficient observation time to fully cover all ∼200,000 *Kepler* targets, except for telescopes with a large number of fibers. In addition, the spectroscopic data from different instruments may suffer systematic uncertainties. Recently, spectroscopic follow-up works in the *Kepler* field for asteroseismolgy have also been performed by the APOKASC with the multiple fibers of SDSS telescope, which is a part of a survey of APOGEE (Majewski et al. 2017; Serenelli et al. 2017; Pinsonneault et al. 2018).

* Based on observations collected with the Large Sky Area Multi-Object Fiber spectroscopic Telescope (LAMOST), which is located at the Xinglong Observatory, China.
[12] Corresponding author.

The Large Sky Area Multi-Object Fiber Spectroscopic Telescope (LAMOST, also known as the Gou Shoujing Telescope) is an ideal instrument for follow-up spectroscopic observations on *Kepler* stars. It combines a large aperture (3.6–4.9 m) with a wide field of view (circular FOV with the diameter of 5°) and is equipped with 4000 fibers at its focus (Wang et al. 1996; Xing et al. 1998). LAMOST spectra have a low-resolution $R \sim 1800$ and cover the wavelength range from 370 to 900 nm (see details in Cui et al. 2012; Zhao et al. 2012). To take advantage of the ability of LAMOST to acquire many spectra at a time over a large field of view, the LAMOST-*Kepler* (LK) project was initiated with the scientific goal to observe as many objects in the *Kepler* FOV as possible from the test and pilot survey phase of LAMOST onward (De Cat et al. 2015, hereafter Paper I). This strategy provides a homogeneous determination of both the atmosphere parameters (i.e., the surface gravity $\log g$, the effective temperature $T_{\rm eff}$, and the metallicity [Fe/H]) and the spectral classification of the observed objects. The low-resolution spectra can also be used to estimate the radial velocity (RV) and the projected rotational velocity ($v \sin i$) for rapid rotation stars.

During the first round of observations, from 2011 May to 2014 September, the LK-project obtained 101,086 low-resolution spectra, covering about 21% of 200,000 *Kepler* stars (Paper I). These spectra were independently analyzed by three different groups: (i) the "Asian team" (Ren et al. 2016) performed a statistical analysis of the stellar parameters based on the LAMOST stellar parameter pipeline (LASP; Wu et al. 2011, 2014; Luo et al. 2015); (ii) the "European team" (Frasca et al. 2016) determined the stellar parameters, the spectral classification, and the activity indicators with an updated version of the code ROTFIT (Frasca et al. 2003, 2006); and (iii) the "American team" (Gray et al. 2016) developed the code MKCLASS, which automatically classifies stellar spectra on the MK system independent of the stellar parameter determination (see details in Gray & Corbally 2014). The LAMOST-*Kepler* spectra, by establishing a spectroscopic database, have made an impact on many scientific areas, particularly for research within the *Kepler* community. These spectra cover the lithium line at 670.8 nm and were used to discover the first confirmed Li-rich core-helium-burning giant (Silva Aguirre et al. 2014). The spectra also cover the Ca II H and K lines at 396.85 and 393.37 nm, respectively, which have been used to measure the chromospheric activity on the stellar surface for 5648 solar-like stars within the *Kepler* field based on LK spectra (Karoff et al. 2016). With the help of LAMOST spectra, the metallicity of the open cluster NGC 6866 has been determined to be similar to the solar value (Bostancı et al. 2015). These spectra are also very useful for individual asteroseismic cases such as the red giant star KIC 5689820 (Deheuvels et al. 2014) and the main-sequence A-type pulsating star KIC 7917485 (Murphy et al. 2016). With the metallicity derived from the LAMOST-*Kepler* spectra, Smalley et al. (2017) found evidence that the incidence of pulsations in Am stars decreases with increasing metallicity. The LAMOST metallicity also plays an important role in the research of *Kepler* exoplanets where an excess of hot rocky *Kepler* planets was found to be preferentially orbiting around metal-rich stars (Mulders et al. 2016) and a new population of short-period ($P < 10$ days) exoplanets with sizes $R_p = 2$–$6\,R_\oplus$ that resemble hot Jupiters was discovered to preferentially occurr around metal-rich hosts and in single-transiting systems. (Dong et al. 2018). With the atmospheric parameters derived from LK-project spectra, stars hosting multiple transiting planets are found with typically near circular or coplanar orbits that are similar to the solar system (Xie et al. 2016), while *Kepler* singles are on average eccentric ($\bar{e} \approx 0.3$). The LK sample is also helpful for investigating the intrinsic architecture of *Kepler* planetary systems, showing that the frequency of *Kepler*-like planetary systems is about 30% (Zhu et al. 2018). In addition, the LK-project is a part of a large spectroscopic survey of Galactic archaeology (see, e.g., Xiang et al. 2017).

Given the importance of these spectra, we report in this paper the second round of spectroscopic observations in the *Kepler* field with the LAMOST telescope from 2015 May to 2017 June. We also include the spectra obtained from the first round of observations, since they are now extracted and analyzed with the most up-to-date pipelines. The structure of this paper is organized as follows. We first describe the details of the observations for this second round in Section 2; the database of this version of the acquired spectra is given in Section 3; a discussion is provided in Section 4; and we end with a brief summary.

## 2. Observations

As LAMOST has a focal plane of 5° in diameter, a minimum of 14 circular LAMOST pointings (or footprints) is needed to cover the 105 square degrees of the *Kepler* field. We refer to these individual footprints as LK-fields and the details of classification of each field can be seen in Paper I. The observed plates are called "V-plates," "B-plates," "M-plates," and "F-plates" for targets with magnitudes of $9 < r \leqslant 14$, $14 < r \leqslant 16.3$, $16.3 < r \leqslant 17.8$, and $17.8 < r \leqslant 18.5$, respectively. In the first round of LK-project observations, we focused on stars that were included on the list of possible targets of the KASC[13] (Paper I). The targets for each plate were selected from a priori tized target list for the second round of observations, compiled from two main types of objects from high to low priority. (1) The 168,151 objects observed by the *Kepler* mission for which no high-quality LAMOST spectrum without potential issues (no entries in column 14 of Table 4 or column 16 of Table 5 of Paper I) was available after the first round of observations, were considered the new "science targets." Within this category, the seismology targets received a higher priority than the planet-search targets. (2) The new "field stars" consisted of three kinds of objects in order of decreasing priority: (a) the 31,567 *Kepler* targets that already have a clean high-quality LAMOST spectrum (to allow multi-epoch observations for quality assessment and variability studies), (b) the objects in the KIC that were not observed by *Kepler*, and (c) other stars in the fields of view with $V < 18$ mag from the USNO-B catalog (Monet et al. 2003). Given the constraints of both the pointing ability of the LAMOST and the visibility of the *Kepler* field, observations can only be done from late May to mid-October with a maximal observation window of four hours. In addition, LAMOST is closed for about two months per year in summer due to the monsoon. Therefore, it takes three or four seasons for LAMOST to achieve full coverage of the whole *Kepler* field, considering the weather conditions as well. Table 1 lists the general information of observations made in each year through the regular survey phase of LAMOST from 2012 to 2017. The multiple visited targets are counted if spectra were

[13] http://www.kasoc.dk

**Table 1**
General Contents of the LK-project Observations during the Regular Survey Phase from 2012 to 2017

| Year | LK Field | Plate | Spectra | Parameter |
|---|---|---|---|---|
| 2012 | 3 | 7 | 17659 | 11682 |
| 2013 | 6 | 14 | 39309 | 28115 |
| 2014 | 7 | 14 | 38516 | 29351 |
| 2015 | 11 | 32 | 97247 | 81381 |
| 2017 | 6 | 16 | 35139 | 23442 |
| Total | | | 227870 | 173971 |
| Unique | | | 104887 | 89570 |
| 2× | | | 37482 | 28077 |
| 3× | | | 10552 | 6613 |
| 4× | | | 2293 | 1429 |
| +5× | | | 1176 | 483 |

**Note.** The number of multiple revisited targets depends on the criteria one chooses when performing cross-identification.

observed with R.A. and decl. within 3.7 arcsec[14] and a magnitude difference less than 0.01 mag. The LK-project has been carried out for two rounds of observations, meaning that all 14 subfields have been observed at least once in each round. We note that the observations during the pilot survey phase of LAMOST have not been processed with the newest version of the pipeline (c.f. Section 3.1) and are not considered here. This study only concerns a small amount of data.

The details of the observations of the first round of the LK-project from 2012 to 2014 are given in Paper I. Here, we focus on the second round of observations of the LK-project, which began on 2015 May 29 and ended on 2017 June 15. A total of 48 plates were observed on 24 observation nights: 32 plates on 18 nights in 2015 and 16 plates on 6 nights 2017. Table 2 provides an overview of the observed plates for the second round of the LK-project. Mainly the very bright "V-plates" were observed, as well as a small fraction of bright "B-plates," with typical exposure times of $3 \times 10$ minutes and $3 \times 25$ minutes, respectively, depending on the observation conditions.

## 3. Spectra Release

### 3.1. Data Reduction Process

One of the main products that LAMOST provides to astronomers is wavelength-calibrated and flux-calibrated spectra, which are processed by an automatic data reduction and data analysis pipeline (see details in Luo et al. 2012, 2015). Pipeline version v2.9.7 is used for spectra obtained during the five-year regular survey of LAMOST from 2012 to 2017. After a quality evaluation of the observations (e.g., seeing and cloud coverage) and telescope performance, the raw CCD frames are fed to the 2D pipeline, which uses procedures similar to those of SDSS (Stoughton et al. 2002), to produce calibrated 1D spectra. The main tasks of the 2D pipeline include dark and bias subtraction, flat=field correction, spectral extraction, sky subtraction, wavelength calibration, stacking sub-exposures and combining of different wavelength bands (a detailed description can be found in Paper I and Luo et al. 2015). The 1D pipeline is aimed at the analysis of the LAMOST spectra and provides classification of spectral type and measurements of RVs (for stars) or redshifts (for galaxies and quasi-stellar objects). This goal is reached with the help of a template-matching and line-recognition algorithm. A library of stellar templates was constructed based on the classification of about one million LAMOST DR1 stellar spectra (Wei et al. 2014).

### 3.2. Data Release

The calibrated spectra are released to the astronomical community at regular intervals, typically once every year, and the pipelines are updated every one or two years, during regular surveys of LAMOST. After two rounds of observations of the LK-project, we have collected 227,870 flux- and wavelength-calibrated, sky-subtracted low-resolution ($R = 1800$) spectra, among which 173,971 spectra have been used to calculate the stellar atmospheric parameters with the LASP pipelines. These data will be released to the public along with the fifth data release (DR5[15]) of all the LAMOST survey spectra in 2019 June. They then can be freely downloaded from the official LAMOST website.[16]

Figure 1 illustrates the spatial distribution of the stars observed within the LK-project from 2012 to 2017. The spatial distribution of the entire data set covers almost the entire area of the *Kepler* field. There are 76,283[17] stars that are both observed by LAMOST and have *Kepler* photometry, corresponding to a fraction of more than a third of the full database of stars observed for the LK-project. We now have LAMOST data for about 38.2% of the ∼200,000 objects that have been observed during the *Kepler* mission. The central hole of each plate is reserved to a bright ($V < 8$) star that is used for the active optics wavefront sensor to shape the mirror getting rid of deformation of the wavefront from external influences. The coordinates of that star also define the coordinates of the observed plate. Four guide stars ($V < 17$) are observed by the guiding CCD cameras placed at the four corners of the LAMOST field of view. Figure 2 shows a histogram of the *Kepler* magnitude (*K*p) distribution for the 146,001 stars, including dwarfs and giants. There are additionally 10,389 stars that are not included among them because they are LAMOST standard stars or stars without *K*p magnitude available from the DR5 catalog. Here, we separate dwarfs from giants by their measured surface gravity with a boundary of $\log g = 3.5$. The histogram of Figure 2 clearly reveals that most targets fall into the range of *K*p 11–14, with a small fraction of brighter and fainter targets. This histogram also depicts the observation strategy of the LK-project under different observation conditions. The observations concentrate on very bright plates (see Table 2, and Table 3 of Paper I), which can make full use of bright nights or nights with unfavorable weather conditions such as poor seeing or low atmospheric transparency. Consequently, a sharp cutoff appears at $K\mathrm{p} = 14$, which is the boundary between the *V*-plates and the *B*-plates.

Figure 3 displays the data quality in terms of the distributions of the signal-to-noise ratios (S/Ns) in the SDSS

[14] This value is adopted on the basis that the fiber pointing precision is 0.4 arcsec and the diameter of the fiber is 3.3 arcsec.

[15] http://dr5.lamost.org

[16] www.lamost.org

[17] This number is obtained through cross-identification between the two data sets on the basis of coordinate separation of 3.0 arcsec. We note that the number would decrease when we used stricter constraints to perform cross-identification. For instance, the number would be around 60,000 if we used a maximum coordinate separation of 0.4 arcsec and a magnitude difference of less than 0.01 mag.

**Table 2**
Overview of the Observed Plates for the Second Round of the LK-project from 2015 to 2017

| PlateID | LK-field | PlanID | R.A. (2000) | Decl. (2000) | Date | Seeing (arcsec) | Exposure Time (s) |
|---|---|---|---|---|---|---|---|
| 3506 | LK14 | KP192323N501616V04 | 19:23:23.787 | +50:16:16.64 | 2015 May 29 | 2.40 | 600 × 3 |
| 3507 | LK14 | KP192323N501616V05 | 19:23:23.787 | +50:16:16.64 | 2015 May 29 | 2.50 | 600 × 2 |
| 3509 | LK11 | KP190651N485531V02 | 19:06:51.499 | +48:55:31.75 | 2015 May 30 | 3.00 | 600 × 3 |
| 3510 | LK11 | KP190651N485531V03 | 19:06:51.499 | +48:55:31.75 | 2015 May 30 | 3.20 | 600 × 3 |
| 3511 | LK11 | KP190651N485531V04 | 19:06:51.499 | +48:55:31.75 | 2015 May 30 | 3.50 | 600 |
| 3538 | LK14 | KP192323N501616B01 | 19:23:23.787 | +50:16:16.64 | 2015 Sep 13 | 4.00 | 1500 × 3 |
| 3542 | LK10 | KP192314N471144B02 | 19:23:14.829 | +47:11:44.80 | 2015 Sep 14 | 3.20 | 1500 × 3 |
| 3544 | LK11 | KP190651N485531B02 | 19:06:51.499 | +48:55:31.75 | 2015 Sep 15 | 2.40 | 1500 × 3 |
| 3546 | LK06 | KP194045N483045B01 | 19:40:45.382 | +48:30:45.10 | 2015 Sep 16 | 3.20 | 1500 × 3 |
| 3551 | LK08 | KP195920N454621B01 | 19:59:20.424 | +45:46:21.15 | 2015 Sep 18 | 3.00 | 1500 × 3 |
| 3552 | LK08 | KP195920N454621B02 | 19:59:20.424 | +45:46:21.15 | 2015 Sep 18 | 3.50 | 1500 + 1356[a] |
| 3599 | LK02 | KP193637N444141V03 | 19:36:37.977 | +44:41:41.77 | 2015 Sep 21 | 3.00 | 600 × 3 |
| 3600 | LK02 | KP193637N444141V04 | 19:36:37.977 | +44:41:41.77 | 2015 Sep 21 | 3.30 | 600 × 3 |
| 3601 | LK02 | KP193637N444141V05 | 19:36:37.977 | +44:41:41.77 | 2015 Sep 21 | 3.90 | 600 × 2 |
| 3620 | LK09 | KP190808N440210V02 | 19:08:08.340 | +44:02:10.88 | 2015 Sep 25 | 3.00 | 600 × 3 |
| 3621 | LK09 | KP190808N440210V03 | 19:08:08.340 | +44:02:10.88 | 2015 Sep 25 | 3.40 | 600 × 3 |
| 3627 | LK06 | KP194045N483045V03 | 19:40:45.382 | +48:30:45.10 | 2015 Oct 01 | 4.20 | 600 × 3 |
| 3628 | LK06 | KP194045N483045V04 | 19:40:45.382 | +48:30:45.10 | 2015 Oct 01 | 4.30 | 600 × 3 |
| 3634 | LK10 | KP192314N471144V02 | 19:23:14.829 | +47:11:44.80 | 2015 Oct 02 | 3.40 | 600 × 3 |
| 3635 | LK10 | KP192314N471144V03 | 19:23:14.829 | +47:11:44.80 | 2015 Oct 02 | 3.80 | 600 × 2 + 561[a] |
| 3642 | LK08 | KP195920N454621V04 | 19:59:20.424 | +45:46:21.15 | 2015 Oct 03 | 2.70 | 600 × 3 |
| 3643 | LK08 | KP195920N454621V05 | 19:59:20.424 | +45:46:21.15 | 2015 Oct 03 | 3.10 | 600 × 3 |
| 3650 | LK12 | KP185031N425443V02 | 18:50:31.041 | +42:54:43.72 | 2015 Oct 04 | 2.80 | 600 × 3 |
| 3658 | LK13 | KP185111N464417V04 | 18:51:11.993 | +46:44:17.52 | 2015 Oct 06 | 4.00 | 600 × 3 |
| 3677 | LK05 | KP194918N413456V04 | 19:49:18.139 | +41:34:56.86 | 2015 Oct 08 | 3.70 | 600 × 3 |
| 3678 | LK05 | KP194918N413456V05 | 19:49:18.139 | +41:34:56.86 | 2015 Oct 08 | 4.70 | 600 × 3 |
| 3679 | LK05 | KP194918N413456V06 | 19:49:18.139 | +41:34:56.86 | 2015 Oct 08 | 2.90 | 600 + 579[a] |
| 3690 | LK07 | KP192102N424113V03 | 19:21:02.816 | +42:41:13.07 | 2015 Oct 11 | 2.80 | 600 × 3 |
| 3691 | LK07 | KP192102N424113V04 | 19:21:02.816 | +42:41:13.07 | 2015 Oct 11 | 3.20 | 600 × 3 |
| 3697 | LK03 | KP192409N391242V01 | 19:24:09.919 | +39:12:42.00 | 2015 Oct 12 | 3.00 | 600 × 3 |
| 3698 | LK03 | KP192409N391242V02 | 19:24:09.919 | +39:12:42.00 | 2015 Oct 12 | 3.60 | 600 × 3 |
| 3731 | LK04 | KP193708N401249V01 | 19:37:08.863 | +40:12:49.63 | 2015 Oct 18 | 4.20 | 600 × 3 |
| 5764 | LK01 | KP190339N395439B01 | 19:03:39.258 | +39:54:39.24 | 2017 Jun 03 | 2.50 | 1500 × 3 |
| 5765 | LK01 | KP190339N395439V03 | 19:03:39.258 | +39:54:39.24 | 2017 Jun 03 | 3.60 | 600 × 2 |
| 5776 | LK12 | KP185031N425443V03 | 18:50:31.041 | +42:54:43.72 | 2017 Jun 07 | 2.50 | 600 × 3 |
| 5777 | LK12 | KP185031N425443V04 | 18:50:31.041 | +42:54:43.72 | 2017 Jun 07 | 2.60 | 600 × 3 |
| 5778 | LK12 | KP185031N425443V05 | 18:50:31.041 | +42:54:43.72 | 2017 Jun 07 | 2.70 | 600 × 4 |
| 5798 | LK04 | KP193708N401249V02 | 19:37:08.863 | +40:12:49.63 | 2017 Jun 12 | 3.20 | 600 × 3 |
| 5799 | LK04 | KP193708N401249V03 | 19:37:08.863 | +40:12:49.63 | 2017 Jun 12 | 3.40 | 600 × 3 |
| 5805 | LK03 | KP192409N391242V03 | 19:24:09.919 | +39:12:42.00 | 2017 Jun 13 | 3.50 | 600 × 3 |
| 5806 | LK03 | KP192409N391242V04 | 19:24:09.919 | +39:12:42.00 | 2017 Jun 13 | 2.70 | 600 × 3 |
| 5807 | LK03 | KP192409N391242V05 | 19:24:09.919 | +39:12:42.00 | 2017 Jun 13 | 2.90 | 600 × 3 |
| 5811 | LK10 | KP192314N471144V04 | 19:23:14.829 | +47:11:44.80 | 2017 Jun 14 | 2.80 | 600 × 3 |
| 5812 | LK10 | KP192314N471144V05 | 19:23:14.829 | +47:11:44.80 | 2017 Jun 14 | 2.90 | 600 × 3 |
| 5813 | LK10 | KP192314N471144V06 | 19:23:14.829 | +47:11:44.80 | 2017 Jun 14 | 3.50 | 600 × 3 |
| 5816 | LK09 | KP190808N440210V04 | 19:08:08.340 | +44:02:10.88 | 2017 Jun 15 | 3.30 | 600 × 3 |
| 5817 | LK09 | KP190808N440210V05 | 19:08:08.340 | +44:02:10.88 | 2017 Jun 15 | 3.70 | 600 × 3 |
| 5818 | LK09 | KP190808N440210V06 | 19:08:08.340 | +44:02:10.88 | 2017 Jun 15 | 4.00 | 600 × 3 |

**Notes.** For each plate, we give the sequence number of the plate (PlateID), the reference of the LK-field (LK#), the plan identification number (PlanID), with the associated right ascension (R.A. (2000)) and declination (decl. (2000)) of the central star on that plate, the observed date (Date), the air turbulence in Xinglong (seeing), and the integral time of each exposure (Exposure time).
[a] The unround exposure time happened due to the plate moving out of the reachable view of LAMOST, two hours before and after its meridian, respectively.

*u, g, r, i*, and *z* bands. We note that the spectra with $S/N_g \geqslant 6$ can be used to derive valid stellar parameters for type A, F, G, and K stars with the LASP pipeline, if they are obtained on dark nights (eight nights before and after the new moon). However, the criterion of $S/N_g$ increases to 15 for the spectra obtained on bright nights (all other nights except the three nights around the full moon). Further details on how those criteria for calculating the atmospheric parameters were established can be found in Luo et al. (2015). After two rounds of LK-project observations, we observed merely 29,505; 40,916; and 53,047 spectra with $S/N_g \leqslant 6$, $S/N_g \leqslant 10$, and $S/N_g \leqslant 15$, observed during both bright and dark

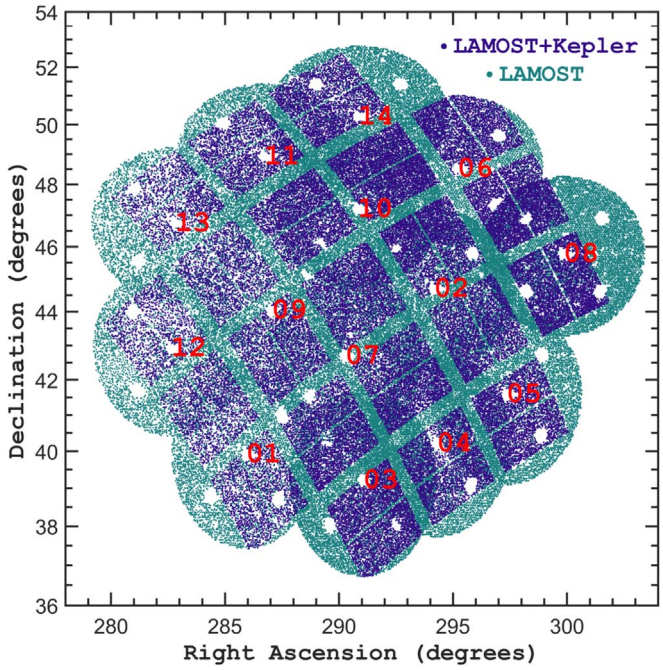


**Figure 1.** Sky coverage of all targets observed by the LK-project. The stars observed by LAMOST and with *Kepler* photometry are dark blue, while others are dark cyan. The numbers mark the central position of the 14 LK fields.

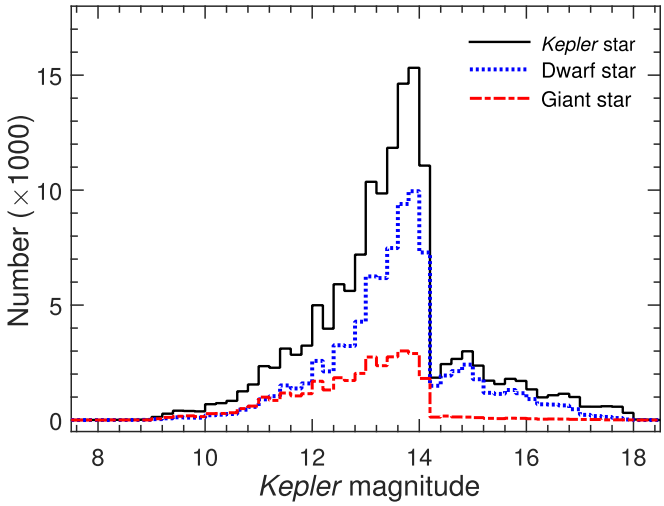


**Figure 2.** *Kepler* magnitude (*Kp*) distribution of the stars observed by LAMOST during the second round of observations. The black solid, blue dotted, and red dashed histograms represent all LK stars (not including the LAMOST standard stars and the stars without an available *Kp* magnitude), the dwarfs, and the giants, respectively.

nights, which correspond to percentages of ∼12.95%, ∼17.96%, and ∼23.28%, respectively.

Table 3 lists the full catalog of the constructed database that is available for the entire LK-project. This table contains the following columns:

Column 1: Obsid is the unique identification number ID of the observed 1D spectrum.
Column 2: the cross-identification of the target in KIC within the coordinate separation of three arcsec.[18]
Column 3: the input target ID from KIC, SDSS, UCAC4, PANSTAR, or another catalog.
Column 4: the input right ascension (epoch 2000.0) of the fiber pointed to, in units of degree.
Column 5: the input declination (epoch 2000.0) of the fiber pointed to, in units of degrees.
Column 6: the $S/N_g$ is the S/N of the spectra in SDSS *g*-band, which gives the quality estimation of the spectrum.
Column 7: the *Kepler* magnitude (*K*p, if available, otherwise the magnitude in a specific filter will be given).
Column 8: subclass is the spectral type of the target calculated by the 1D pipeline if they are stars of A, F, G, K, and M types.
Column 9: the effective temperature with the associated error given by the LASP pipeline ($T_{\rm eff}$).
Column 10: the surface gravity with the associated error given by the LASP pipeline ($\log g$).
Column 11: the metallicity with the associated error given by the LASP pipeline.
Column 12: the RV with the associated error given by the LASP pipeline.
Column 13: the (local) observation time of the spectrum.
Column 14: the coordinate difference between the observed coordinates of LAMOST and the cross-identification from KIC coordinates (in arcsec).
Column 15: the availability of *Kepler* photometry ("Y" for yes and "N" for no).
Column 16: the file name of the LAMOST 1D fits file.

[18] We note that the criteria are different for cross-identification and self-identification (c.f. Section 2). The nearest star will be chosen if more than one star is identified.

### 3.3. Characterization of Atmospheric Parameters

Among these 227,870 spectra, we provide stellar parameters for 173,971 spectra with the LASP pipeline, as the spectra quality is high enough to achieve an accurate and reliable determination of the parameters for the AFGK-types of stars (with $S/N_g \geqslant 6$ and $S/N_g \geqslant 15$ of spectra observed on dark and bright nights, respectively; see Luo et al. 2015 for more details). We note that 51,503 targets have been observed more than once (16× for the most observed stars) and the total number of stars is 156,390. There are 65,529 *Kepler* stars with LASP atmospheric parameters among the 76,283 stars in common. We now have LASP parameters for about 32.8% of the objects that have been observed during the *Kepler* mission. Figure 4 shows the $\log g$ versus $T_{\rm eff}$ plane (also called a Kiel diagram) for the spectra with sufficient quality. The distribution of targets differs slightly but not significantly, therefore it is not provided here again. The surface gravities are found mainly between 5 and 1 dex, while the effective temperature is mainly in the range of [4000, 8000] K. Most stars have metallicities near the value of the Sun. We clearly see that most of them are located on either the main-sequence or the red giant branch. We note that the giant branch correctly displaces toward higher temperatures as the metallicity decreases.

Figure 5 shows histograms of the stellar parameters $T_{\rm eff}$, $\log g$, [Fe/H], and the RV. The distribution of effective temperature, $T_{\rm eff}$, shows a structure where two distinct peaks are found around 4700 and 5700 K, which are projections of the giants and the main-sequence stars from Figure 4, respectively. The surface gravity, $\log g$, also presents two distinct peaks near 2.5 and 4.2 which, again, correspond to the projection of the giant and the main-sequence stars, respectively. The metallicity spans the range from ∼−2.0 to 0.7 dex

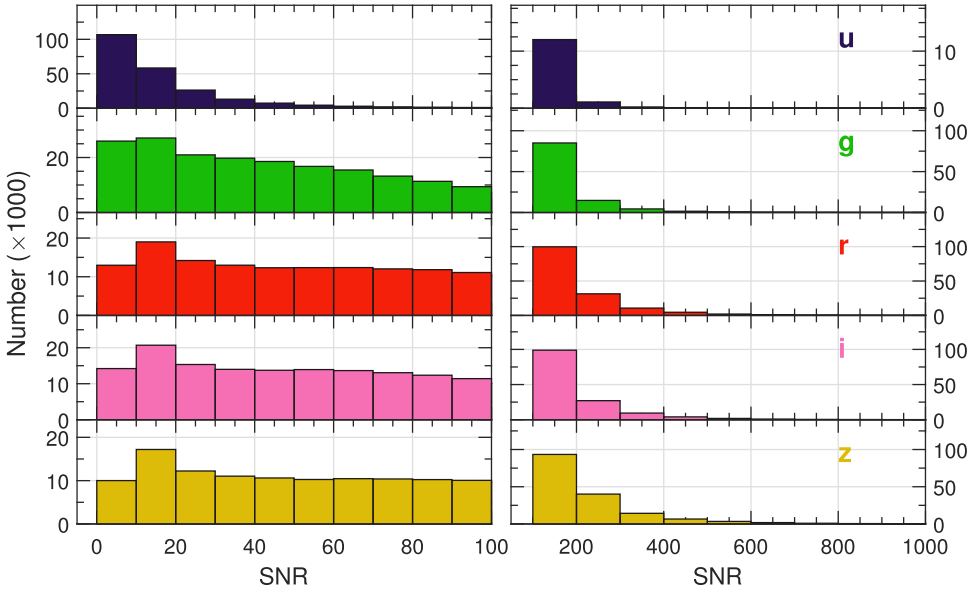


**Figure 3.** Distributions of the S/N in the SDSS *u*, *g*, *r*, *i*, and *z* bands (from the top down to the bottom panels) for the LK spectra. The left and right panels show the S/N ranges [0, 100] and [100, 1000], with bin sizes 10 and 100, respectively.

and peaks around the solar metallicity, which suggests that most stars have a nearly solar metallicity. There are 1114 stars with [Fe/H] $< -1.0$ and 65 stars with [Fe/H] $< -2.0$, which we consider as candidate metal-poor stars and very-metal-poor stars, respectively. They could be fossils of the early generation of stars and can provide fundamental information on the chemical abundances, formation, and evolution of the early evolutionary stage of the Galaxy (see, e.g., McWilliam et al. 1995; Li et al. 2015). Most stars are found with RVs around $-20\,\mathrm{km\,s^{-1}}$. However, in the long tail of the RV distribution, we find 29 and 216 stars with RV $< -400\,\mathrm{km\,s^{-1}}$ and $-300\,\mathrm{km\,s^{-1}}$, which are candidates of high-velocity stars (see, e.g., Zhong et al. 2014). The properties of these stars can be used to determine their original nature and their formation mechanisms and aid the study of the structural properties of the Galaxy (see, e.g., Gvaramadze et al. 2009).

## 4. Discussion

After completing both rounds of observations of the LK-project, we have collected 227,870 low-resolution spectra of 156,390 stars and provided atmospheric parameters with 173,971 spectra of 126,172 stars. We remark that the low-resolution spectra in the first round of observations were mainly produced from the LASP pipeline with version 2.7.5. The parameter comparison from those two versions is reported in the data release note of the DR5 website,[19] where it is shown that the atmospheric parameters $T_{\rm eff}$, $\log g$, [Fe/H], and RV are within their errors for the stars in common between DR3 and DR5. We note that for stars within the LK-project, the parameters are also essentially the same, as displayed by the similarity of Figure 6 in Paper I to Figures 4 and 5 here. The slight difference between the two Kiel diagrams is mainly the result of excluding from the analysis the parameters of hot stars (OB-types) because the LASP pipeline is optimized for AFGK-type stars and could lead to untrustworthy results in other cases. Nevertheless, as the size of the sample has increased, we have observed more interesting targets such as candidates of very-low-metallicity stars and high-velocity stars (see Figure 6 of Paper I and Figure 5).

For the spectral database of only the first round of the LK-project, Ren et al. (2016) calibrated the atmospheric parameters derived from LASP by comparing them with the values measured from either high-resolution spectroscopy or asteroseismology for the stars in common with the catalog of Huber et al. (2014). A similar comparison was also performed by Dong et al. (2014, 2018) and Wang et al. (2016). Ren et al. (2016) provided external errors of $T_{\rm eff}$, $\log g$, and [Fe/H] for giants and dwarfs, respectively. Internal errors have also been estimated with values derived from multiple spectra of the same stars. A forthcoming paper (Y. Pan et al. 2018, in preparation) will focus on the same topic with a database more than twice the previous spectral library, from 61,226 to 173,971. The number of common stars that have been observed by both *Kepler* and LAMOST is 76,283, a number larger than twice the data size of Ren et al. (2016). In addition, the previous spectra have been reanalyzed with the updated version of the LASP code, v2.9.7, where the determination of uncertainty of RV is improved significantly. The new calibration examines the reliability of the previous results provided by Ren et al. (2016), to establish more generic calibration formulae.

Other groups, including the "European" and "American" teams, are applying their own codes to these spectra for the determination of basic stellar parameters. The "European team" (J. Molenda-Żakowicz et al. 2019, in preparation) is determining the atmospheric parameters, the spectral classification, the projected rotational velocity (for ultrafast rotators only), and activity indicators with the latest adapted version of the code ROTFIT, for the entire database extending the results of their previous work (Frasca et al. 2016). The "American team" (R. O. Gray et al. 2018, in preparation) is performing an accurate MK classification with the automatic code MKCLASS, which is independent of the determination of atmospheric parameters (see details in Gray et al. 2016).

The current LASP and the above pipelines have not yet incorporated the templates for hot and highly evolved stars,

[19] http://dr5.lamost.org/doc/release-note

**Table 3**
Database of the LAMOST Spectra Obtained for the LK-project from 2012 to 2017

| (1) | (2) | (3) | (4) | (5) | (6) | (7) | (8) |
|---|---|---|---|---|---|---|---|
| Obsid[a] | KIC[b] | Tcomment | R.A. (2000) | Decl. (2000) | $S/N_g$ | Mag | Subclass |
| (9) | (10) | (11) | (12) | (13) | (14) | (15) | (16) |
| $T_{\rm eff}$ (K) | $\log g$ (dex) | [Fe/H] (dex) | RV (km $s^{-1}$) | yyyy-mm-ddThh:mm:ss.ss | $\Delta d$ (arcsec) | KO | Filename |
| … | … | … | … | … | … | … | … |
| … | … | … | … | … | … | … | … |
| 580608079 | 3958615 | kplr003958615 | 292.6349200 | 39.02463200 | 111.19 | 12.80 | G5 |
| 4272.48 ± 24.10 | 2.159 ± 0.040 | −0.399 ± 0.022 | −30.37 ± 3.46 | 2017 Jun 14T02:06:16.0 | 0.028878 | Y | spec-57918-KP192409N391242V04_sp08-079.fits.gz |
| 580608081 | 3958237 | kplr003958237 | 292.5281700 | 39.08282100 | 83.08 | 13.71 | G5 |
| 4773.65 ± 29.01 | 2.509 ± 0.048 | −0.170 ± 0.027 | −8.53 ± 3.65 | 2017 Jun 14T02:06:16.0 | 0.029562 | Y | spec-57918-KP192409N391242V04_sp08-081.fits.gz |
| 580608082 | 3957804 | 1275-11519892 | 292.4251750 | 39.04117800 | 30.22 | 13.20 | G3 |
| 5828.24 ± 88.58 | 4.174 ± 0.145 | 0.201 ± 0.086 | −43.62 ± 5.91 | 2017 Jun 14T02:06:16.0 | 2.88 | Y | spec-57918-KP192409N391242V04_sp08-082.fits.gz |
| 580608084 | 3958877 | kplr003958877 | 292.7043500 | 39.02043200 | 125.91 | 13.23 | G2 |
| 5816.16 ± 18.31 | 4.028 ± 0.030 | 0.119 ± 0.017 | −21.41 ± 4.27 | 2017 Jun 14T02:06:16.0 | 0.027528 | Y | spec-57918-KP192409N391242V04_sp08-084.fits.gz |
| 580608086 | 3958406 | kplr003958406 | 292.5780000 | 39.03916900 | 38.67 | 13.92 | G3 |
| 5883.81 ± 61.31 | 4.449 ± 0.101 | 0.103 ± 0.059 | −29.80 ± 6.01 | 2017 Jun 14T02:06:16.0 | 0.02958 | Y | spec-57918-KP192409N391242V04_sp08-086.fits.gz |
| … | … | … | … | … | … | … | … |
| … | … | … | … | … | … | … | … |

**Notes.** The entire table can be downloaded from dr5.lamost.org/doc/vac.
[a] Obsid is the "fingerprint" of that spectrum. One can keep the obsid if seeking more information on that spectrum. It can be easily accessed though the official LAMOST website search engine: dr5.lamost.org/search.
[b] One should be careful when using the KIC identification if it has a large separation $\Delta d$ or conflicts with its tcomment (input target).

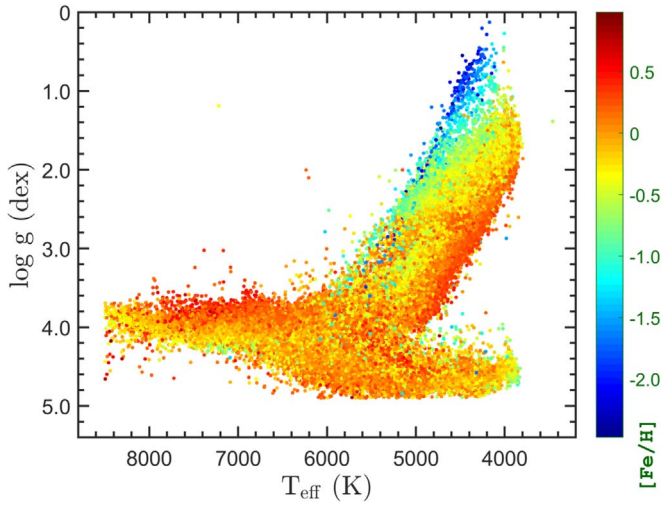


**Figure 4.** Kiel diagram ($\log g$ vs. $T_{\rm eff}$) of the qualified LK spectra. The parameters are derived from the LASP pipeline. Note that different colors indicate different values of metallicity [Fe/H].

including the O and B type main-sequence stars, the white dwarfs, and the hot subdwarf stars. With the previous LAMOST data (including the LK-project's), several independent works have concentrated on highly evolved compact stars, aiming to characterize and determine the stellar parameters of white dwarfs (Zhao et al. 2013; Guo et al. 2015), as well as hot subdwarfs (Luo et al. 2016). These stars, which are not analyzed by the LASP code, are scientifically valuable when their parameters are derived by specialized outside pipelines or models (see, e.g., Su et al. 2017).

In line with the initial goals for the LK-project, there are fruitful results being generated based on this catalog, together with the *Kepler* photometry. During in-depth study of *Kepler* targets based on the full database, a cross-identification was established between the catalog of the LAMOST DR4/DR5 and the *Kepler* archive, with a tolerance of three arcsec in coordinate separation (A. Luo et al. 2018 in preparation), which is useful for determining the contamination factor of the targets that are affected by their neighbor sources during the *Kepler* observations (see also Table 5 of Paper I, which lists this value for the DR3 data). For stars with large contamination factors, one should be extremely careful since those targets may be very close to their neighbor objects and a star wrongly observed by LAMOST cannot be ruled out.

The astronomical community can exploit the spectra of this database for research in many different fields, such as stellar activity, binaries, and asteroseismology. Yang et al. (2017) provided a comprehensive investigation of stellar flare events in M dwarfs in the *Kepler* field with the H$\alpha$ emission lines illustrated from the LAMOST spectra. There are 483 stars with multiple (5+) spectra that can be used to check the variations of RVs, serving as an independent technique to discover new binary systems and to solve their orbital parameters (see, e.g., Catanzaro et al. 2018). A major goal of the LK-project is to provide accurate parameters for pulsating stars, since their pulsations can be measured to a precision of a few tenths of a nanohertz from the *Kepler* photometry (see, e.g., Zong et al. 2016), which are key input parameters for the seismic modeling of pulsating stars.

A drawback of the LK-project is that the *Kepler* original field can only be reached by LAMOST during the summer season when the weather conditions produce high precipitation due to the Monsoon (Paper I). Therefore, to fully extend the capacity of LAMOST, providing spectra for targets with high-quality photometry, we select six *K2* campaigns (i.e., C0, C1, C4, C5, C6, and C8; Howell et al. 2014) whose declinations are higher than $-10^{\circ}$, and hence reachable by LAMOST to carry out the LAMOST-*K2* project observations. Each field is divided into 14 subfields, similar to the LK subfields. During a period from 2014 to 2017, a total of 151 plates were observed over 108 nights, with a collection of 291,956 spectra for 222,926 stars (J. Wang et al. 2018, in preparation). The calibration of $\log g$ between the asteroseismic determination and the LASP code was obtained by R. Zhang et al. (2018, in preparation). We also note that a current proposal of LAMOST has been approved for follow-up observations on the region near the north ecliptic pole, where the *TESS* mission will observe continuously with a duration of about one year (Ricker et al. 2014).

As LAMOST finished its first five-year regular survey in 2017 summer, several interesting proposals were approved, in particular observations related to the LK-project. One of them is the time-series spectroscopic observations for the targets in the field of *Kepler* and *K2*, with 16 middle-resolution ($R \sim 7500$) spectrographs but for two different arms, with wavelength ranges of 630–680 nm and 495–535 nm, respectively. Observations of the test plate (i.e., LK07) were completed on 2018 May 24 and 28–31. The preliminary data set of parameters contains about 1800 targets, with most of them revisited 30 times. A forthcoming paper will concentrate on the test results. All the data will be available publicly after 2020 September, along with the DR6.

## 5. Summary

The LK-project, in support of follow-up spectroscopic observations for *Kepler* photometry, aims to provide spectra for investigating the variety of physics conditions of the stars observed by *Kepler*. During the first five-year regular survey phase, the original *Kepler* field has been observed by LAMOST on 83 plates over 49 nights from 2012 June to 2017 June, accumulating 227,870 spectra of 156,390 stars. From the cross-identification of ~200,000 targets with available *Kepler* photometry, we find 76,283 stars in common between LAMOST and *Kepler* with constraints on the coordinate separation ($d < 3.0$ arcsec).

At the current stage, we have obtained stellar parameters with 173,971 spectra of 126,172 stars of type A, F, G, and K star with the LASP pipeline v2.9.7, which provide hundreds of candidate high-velocity stars and metal-poor or very-metal-poor stars. A process of homogenization between our data and the products of other works is ongoing. This work will provide us with a more robust estimation of the derived parameters. These spectra will be useful for the entire astronomical community, particularly for investigating planetary science and the stellar physics of *Kepler* targets.

Although LAMOST has completed its first five-year regular survey, the LK-project will be continued in the future to provide more spectra. In parallel to the LK-project, there are several approved programs to use LAMOST for follow-up observations of the targets of operating and forthcoming space missions such as *K2* and *TESS* satellites. In order to provide time-series spectroscopy, one footprint on the *K2* C0 field has been continuously observed more than 10 times. A very similar project is under test while LAMOST is equipped with

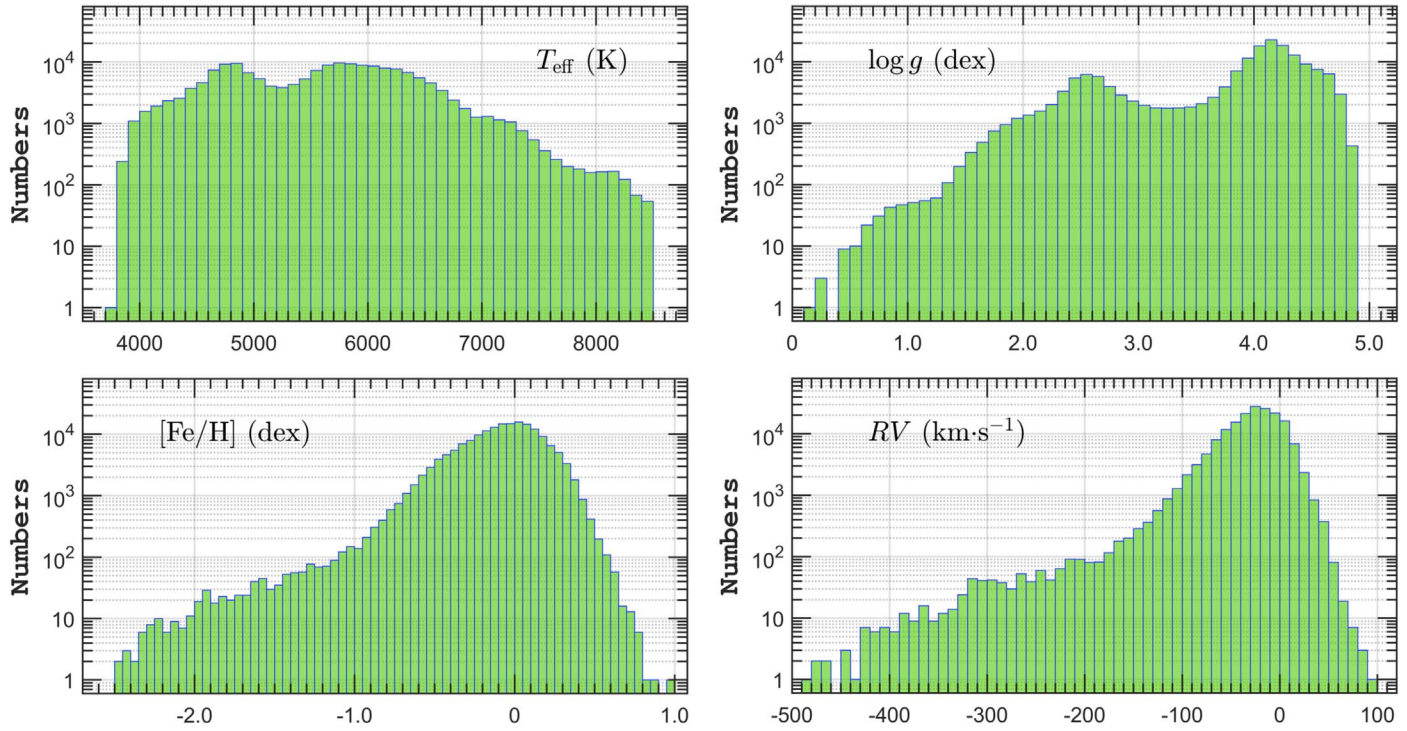


**Figure 5.** Histogram of atmospheric parameters derived from 173,971 spectra. Top left panel: the effective temperature $T_{\rm eff}$ (K, with a bin of 100 K); top right: the surface gravity log $g$ (dex, with a bin of 0.1); bottom left: the metallicity [Fe/H] (dex, with a bin of 0.05); and bottom right: the radial velocity RV (km s$^{-1}$, with a bin of 10 km s$^{-1}$).

intermediate-resolution spectrographs. Astronomers who are interested in those spectra can contact the members of the LAMOST consortium.[20]

The Guoshoujing Telescope (the Large Sky Area Multi-object Fiber Spectroscopic Telescope LAMOST) is a National Major Scientific Project built by the Chinese Academy of Sciences. Funding for the project has been provided by the National Development and Reform Commission. LAMOST is operated and managed by the National Astronomical Observatories, Chinese Academy of Sciences. W.K.Z. hosts the LAMOST fellowship as a Youth Researcher, supported by Special Funding for Advanced Users, and budgeted and administered by the Center for Astronomical Mega-Science, Chinese Academy of Sciences (CAMS). W.K.Z., J.N.F., Y.P., R.Y.Z., J.T.W., and M.Q.J. acknowledge the support from the National Natural Science Foundation of China (NSFC) through grants 11673003, 11833002, and the National Basic Research Program of China (973 Program 2014CB845700). J.M.-Ż. acknowledges the Polish National Science Centre grant No. 2014/13/B/ST9/00902 and the Wroclaw Centre for Networking and Supercomputing grant No.224. S.D. acknowledges Project 11573003 supported by NSFC and the LAMOST Fellowship, which is supported by Special Funding for Advanced Users, budgeted and administered by CAMS. The work presented in this paper is supported by the project "LAMOST Observations in the *Kepler* field" (LOK), approved by the Belgian Federal Science Policy Office (BELSPO, Govt. of Belgium; BL/33/FWI20).

*Software:* LASP (v2.9.7; Wu et al. 2011; Luo et al. 2015).

[20] Send requests to Dr. Ali Luo (lal@bao.ac.cn).

## ORCID iDs

Weikai Zong https://orcid.org/0000-0002-7660-9803
Jian-Ning Fu https://orcid.org/0000-0001-8241-1740
Peter De Cat https://orcid.org/0000-0001-5419-2042
Jianrong Shi https://orcid.org/0000-0002-0349-7839
Haotong Zhang https://orcid.org/0000-0002-6617-5300
C. J. Corbally https://orcid.org/0000-0001-6797-887X
Subo Dong https://orcid.org/0000-0002-1027-0990

## References

Borucki, W. J., Koch, D., Basri, G., et al. 2010, Sci, 327, 977
Bostancı, Z. F., Ak, T., Yontan, T., et al. 2015, MNRAS, 453, 1095
Brown, T. M., Latham, D. W., Everett, M. E., & Esquerdo, G. A. 2011, AJ, 142, 112
Catanzaro, G., Frasca, A., Giarrusso, M., et al. 2018, MNRAS, 477, 2020
Charpinet, S., Van Grootel, V., Fontaine, G., et al. 2011, A&A, 530, A3
Cui, X.-Q., Zhao, Y.-H., Chu, Y.-Q., et al. 2012, RAA, 12, 1197
Cunha, M. S., Aerts, C., Christensen-Dalsgaard, J., et al. 2007, A&ARv, 14, 217
De Cat, P., Fu, J. N., Ren, A. B., et al. 2015, ApJS, 220, 19
Deheuvels, S., Doğan, G., Goupil, M. J., et al. 2014, A&A, 564, A27
Doi, M., Tanaka, M., Fukugita, M., et al. 2010, AJ, 139, 1628
Dong, S., Xie, J.-W., Zhou, J.-L., Zheng, Z., & Luo, A. 2018, PNAS, 115, 266
Dong, S., Zheng, Z., Zhu, Z., et al. 2014, ApJL, 789, L3
Frasca, A., Alcalá, J. M., Covino, E., et al. 2003, A&A, 405, 149
Frasca, A., Guillout, P., Marilli, E., et al. 2006, A&A, 454, 301
Frasca, A., Molenda-Żakowicz, J., De Cat, P., et al. 2016, A&A, 594, A39
Gilliland, R. L., Brown, T. M., Christensen-Dalsgaard, J., et al. 2010, PASP, 122, 131
Gray, R. O., & Corbally, C. J. 2014, AJ, 147, 80
Gray, R. O., Corbally, C. J., De Cat, P., et al. 2016, AJ, 151, 13
Guo, J., Zhao, J., Tziamtzis, A., et al. 2015, MNRAS, 454, 2787
Gvaramadze, V. V., Gualandris, A., & Portegies Zwart, S. 2009, MNRAS, 396, 570
Howell, S. B., Sobeck, C., Haas, M., et al. 2014, PASP, 126, 398
Huber, D., Silva Aguirre, V., Matthews, J. M., et al. 2014, ApJS, 211, 2
Karoff, C., Knudsen, M. F., De Cat, P., et al. 2016, NatCo, 7, 11058

Li, H.-N., Zhao, G., Christlieb, N., et al. 2015, ApJ, 798, 110
Luo, A.-L., Zhang, H.-T., Zhao, Y.-H., et al. 2012, RAA, 12, 1243
Luo, A.-L., Zhao, Y.-H., Zhao, G., et al. 2015, RAA, 15, 1095
Luo, Y.-P., Németh, P., Liu, C., Deng, L.-C., & Han, Z.-W. 2016, ApJ, 818, 202
Majewski, S. R., Schiavon, R. P., Frinchaboy, P. M., et al. 2017, AJ, 154, 94
McNamara, B. J., Jackiewicz, J., & McKeever, J. 2012, AJ, 143, 101
McWilliam, A., Preston, G. W., Sneden, C., & Searle, L. 1995, AJ, 109, 2757
Molenda-Żakowicz, J., Latham, D. W., Catanzaro, G., Frasca, A., & Quinn, S. N. 2011, MNRAS, 412, 1210
Monet, D. G., Levine, S. E., Canzian, B., et al. 2003, AJ, 125, 984
Mulders, G. D., Pascucci, I., Apai, D., Frasca, A., & Molenda-Żakowicz, J. 2016, AJ, 152, 187
Murphy, S. J., Bedding, T. R., & Shibahashi, H. 2016, ApJL, 827, L17
Niemczura, E., Murphy, S. J., Smalley, B., et al. 2015, MNRAS, 450, 2764
Pinsonneault, M. H., Elsworth, Y. P., Tayar, J., et al. 2018, arXiv:1804.09983
Prša, A., Batalha, N., Slawson, R. W., et al. 2011, AJ, 141, 83
Ren, A., Fu, J., De Cat, P., et al. 2016, ApJS, 225, 28
Ricker, G. R., Winn, J. N., Vanderspek, R., et al. 2014, Proc. SPIE, 9143, 914320
Serenelli, A., Johnson, J., Huber, D., et al. 2017, ApJS, 233, 23
Silva Aguirre, V., Ruchti, G. R., Hekker, S., et al. 2014, ApJL, 784, L16
Smalley, B., Antoci, V., Holdsworth, D. L., et al. 2017, MNRAS, 465, 2662
Stoughton, C., Lupton, R. H., Bernardi, M., et al. 2002, AJ, 123, 485
Su, J., Fu, J., Lin, G., et al. 2017, ApJ, 847, 34
Thygesen, A. O., Frandsen, S., Bruntt, H., et al. 2012, A&A, 543, A160
Uytterhoeven, K., Briquet, M., Bruntt, H., et al. 2010, AN, 331, 993
Wang, L., Wang, W., Wu, Y., et al. 2016, AJ, 152, 6
Wang, S.-G., Su, D.-Q., Chu, Y.-Q., Cui, X., & Wang, Y.-N. 1996, ApOpt, 35, 5155
Wei, P., Luo, A., Li, Y., et al. 2014, AJ, 147, 101
Wu, T., Du, B., Luo, A., Zhao, Y., & Yuan, H. 2014, in IAU Symp. 306, Statistical Challenges in 21st Century Cosmology (Cambridge: Cambridge Univ. Press), 340
Wu, Y., Singh, H. P., Prugniel, P., Gupta, R., & Koleva, M. 2011, A&A, 525, A71
Xiang, M.-S., Liu, X.-W., Shi, J.-R., et al. 2017, MNRAS, 464, 3657
Xie, J.-W., Dong, S., Zhu, Z., et al. 2016, PNAS, 113, 11431
Xing, X., Zhai, C., Du, H., et al. 1998, Proc. SPIE, 3352, 839
Yang, H., Liu, J., Gao, Q., et al. 2017, ApJ, 849, 36
Zhao, G., Zhao, Y.-H., Chu, Y.-Q., Jing, Y.-P., & Deng, L.-C. 2012, RAA, 12, 723
Zhao, J. K., Luo, A. L., Oswalt, T. D., & Zhao, G. 2013, AJ, 145, 169
Zhong, J., Chen, L., Liu, C., et al. 2014, ApJL, 789, L2
Zhu, W., Petrovich, C., Wu, Y., Dong, S., & Xie, J. 2018, ApJ, 860, 101
Zong, W., Charpinet, S., Vauclair, G., Giammichele, N., & Van Grootel, V. 2016, A&A, 585, A22